Journal of Electronics and Electrical Engineering
https://ojs.wiserpub.com/index.php/JEEE

Research Article

Sizing Optimization and Economic Modeling of a Stand-alone Hybrid Power System for Supplying RO System in McCallum

Fatemeh Kafrashi*, Tariq Iqbal

Department of Electrical and Computer Engineering, Memorial University of Newfoundland, St. John's, NL, Canada
E-mail: fkafrashi@mun.ca

Received: 27 June 2024; **Revised:** 26 August 2024; **Accepted:** 27 August 2024

Abstract: Access to potable water has always been a fundamental human need. However, climate changes and water contamination are now exacerbating its scarcity. Consequently, the desalination of existing water sources has become increasingly critical. A reverse osmosis (RO) treatment system was employed in this study due to its lower energy consumption compared to other methods and its high effectiveness in removing lead from water. We aimed to provide electricity for a water system serving the remote community of McCallum in Newfoundland and Labrador. McCallum faces water shortages and lead contamination issues, and due to its isolated location, it remains disconnected from the electricity grid. To address this, we designed a hybrid energy system (HES) capable of supplying the necessary electricity for the water system. After conducting an economic analysis, we proposed the most optimal configuration using Homer Pro software. This configuration includes 3.19 kW PV panels, a 2-kW wind turbine, a 3-kW diesel generator, and 32.3 kWh batteries. The optimized system has a net present cost (NPC) of $44,382, which is 3.4 times less than that of the diesel-only system with an NPC of $153,940. Additionally, we investigated the system's sensitivity to changes in diesel prices and the annual average load to observe its behavior. This paper offers a reliable and environment-friendly HES for the water system in McCallum.

Keywords: hybrid energy system, water desalination, reverse osmosis, economic analysis, HOMER Pro, PV/WT/diesel/battery systems

Nomenclature

AHP	(Analytic Hierarchy Process)
ALARA	(As Low As Reasonably Achievable)
AO	(Aesthetic Objective)
BWD	(Brackish Water Desalination)
CC	(Charge Controller)
CDM	(Canadian Drought Monitor)
COE	(Cost of Energy)
ED	(Electrodialysis)

DOI: https://doi.org/10.37256/jeee.3220245201

EIs	(Environmental Impacts)
EPA	(United States Environmental Protection Agency)
GHG	(Green House Gases)
GHI	(Global Horizontal Irradiance)
HES	(Hybrid Energy System)
MAC	(Maximum Acceptable Concentration)
MED	(Multi-effect Distillation)
MSF	(Multi-stage Flash Distillation)
MVC	(Mechanical Vapor Compression)
NPC	(Net Present Cost)
NTUs	(Nephelometric Turbidity Units)
OG	(Operational Guidance Value)
POWER	(NASA Prediction of Worldwide Energy Resource)
RES	(Renewable Energy Sources)
RO	(Reverse Osmosis)
STC	(Standard Test Conditions)
SWD	(Seawater Desalination)
SWST	(Seasonal Water Storage Tank)
TCUs	(True Colour Units)
TVC	(Thermal Vapor Compression)
WHO	(World Health Organization)
WWAP	(United Nations World Water Assessment Programme)

1. Introduction

Potable water has always been a critical source all over the world. Even though about 70% of the earth is covered by water, only 1% is accessible freshwater [1]. The demand for water continues to escalate owing to the growing needs of diverse sectors like agriculture, industry, and municipality. The United Nations World Water Assessment Programme (WWAP) has estimated that by 2030, only 60 percent of the global water requirement will be met. Additionally, the impact of climate change and water contamination will serve as significant barriers to accessing potable water sources [2]. In 2010, It was acknowledged by the United Nations General Assembly that access to water is the right of all human beings [2]. Due to its technical and financial feasibility, increasing demand and the limited resources for fresh water make desalination a more reliable option for worldwide water supply [3].

Desalination is categorized into two main types- seawater desalination (SWD) or brackish water desalination (BWD) [4], Desalination technology needs a significant amount of energy that leads to an increase in energy demands [5]. Reverse osmosis (RO) is currently the most prevalent desalination method worldwide [6]. Environmental impacts (EIs) caused by the desalination process are mainly because of discharges of brine water [7]. Furthermore, if the necessary energy is intended to be provided by burning fossil fuels, increasing desalination systems capacity will lead to more greenhouse gases (GHG) releases [8]. To avoid this, different renewable energy sources (RES) have the potential to be combined with desalination processes [7].

These RES-based desalination plants are typically established in decentralized locations where power supply from public utility grids is not feasible. Often, these decentralized systems are hybrid integrated units, combining multiple renewable energy sources such as wind and solar, solar and geothermal, or solar and biomass in conjunction with diesel generators. Energy storage devices are added to guarantee an uninterrupted power supply [9].

Various papers have studied the configurations of hybrid energy sources supplying the required electricity for RO systems. Table 1 (left) and 1 (right) in this paper compares features, analytical tools, and methods of different configurations for hybrid energy systems, summarizing these studies. Novosel et al. studied the economic and environmental feasibility of implementing wind and solar energies with an RO system in Jordan. The flexibility of the desalination system significantly

enhances the potential for integrating intermittent RES, thereby reducing total annual fuel consumption, overall system costs, and CO_2 emissions [10]. Dawood et al. developed a solar-powered, battery-free RO plant in Egypt. It treats brackish water with up to 25,000 TDS and produces 1000 cubic meters of drinkable water per day at an estimated cost of $0.55 to $0.63 per cubic meter. Using GIS technology, they selected an optimal location [11]. While economical, the drawback is reliance on solar irradiance, affecting water production during low sunlight. Ajiwiguna et al. introduced a PV-RO system with a seasonal water storage tank (SWST) to extend water production and minimize energy waste. By incorporating SWST, the required battery capacity decreases. The cost of water production decreased significantly, from $10.21 to $2.31 per cubic meter (steady requirements) and from $36.96 to $3.06 per cubic meter (fluctuating requirements), when comparing PV-RO-Battery structures with and without SWST [12]. Wu et al. optimized a hybrid PV-diesel-battery system for RO desalination in Iran using Tabu search. The life cycle cost was $28,130. Desalinated water cost ranged from $1.59 to $2.39 per cubic meter, and the levelized energy cost was $0.3975 to $0.5975 per kWh. The hybrid system outperformed individual diesel or PV systems economically and environmentally [13]. Alsheghri et al. investigated a PVRO system for the Masdar Institute in Dubai. They opted for direct power supply from the grid, using PV to produce energy for RO. This approach eliminates costly batteries and extra land, reducing the government water production subsidies by 84% [14]. Kabir et al. developed a cost-efficient PVRO system to purify brackish underground water on the isolated island of Sandwip in Bangladesh. The purified water meets WHO and Bangladesh standards, with a salinity of 233 mg/L. The system's water purification cost is $0.002 per liter, making it more economical than bottled water setups. The energy cost is $0.13 per kWh, providing a financially sensible solution compared to other power production options in the area [15]. Genai et al. investigated power system architectures for an agricultural farm and RO system. The grid-tied system, combining solar PV production with grid energy, emerged as the optimal choice. It achieved the lowest life cycle cost of electricity generation ($85/MWh), a high renewable fraction (67%), and minimal CO_2 emissions (208 kg per MWh). The grid-tied configuration provides an environmentally friendly and cost-effective solution [16]. In their study, Mousavi et al. optimized a standalone hybrid PV system to supply power to a house with an RO system in Sinak village, Iran. They considered two scenarios: (1) a PV system with battery storage and (2) a PV system with battery storage and a gas generator. The cost analysis revealed a net present cost (NPC) of $10,245 and a cost of energy (COE) of $0.31 per kWh for the PV-battery-RO system. Despite higher upfront costs, this environmentally friendly system operates with zero carbon emissions and offers extended up to 100 h of autonomy. Additionally, it has a simplified control system because of the charge controller (CC) dispatch strategy and less system elements [17].

Existing hybrid energy system (HES) configurations for RO systems face significant challenges, including heavy reliance on solar irradiance, high initial costs, and critical energy storage issues. In cold remote locations, the lack of grid connection and impracticality of SWST due to freezing temperatures further complicate implementation. The proposed HES configuration aims to address these issues by combining renewable energy sources with diesel generators and batteries as backup systems to ensure 24/7 operation. This system is designed to supply a submersible pump that extracts water from a drilled well and an RO system designed to provide clean drinking water for the people of McCallum in Newfoundland and Labrador, Canada, using Homer Pro software. The proposed system combines energy sources, including solar and wind, with a battery and diesel generator as backup systems to meet the load requirement in case of wind and solar resource shortages. Section 2 provides some details about water quality standards and desalination methods. Section 3 presents site identification and details about electric load demand, Section 4 explains climatic data and components of the hybrid power system in detail and technically, Section 5 provides economic and operational results simulation, and Section 6 elaborates on the conclusion of the study.

Table 1 (left). Literature review

Authors/Year	Grid	PV	Wind	BAT	DG	RO	Other Load	Location	Analytical Tools or Methods
Novosel et al./2015 [10]		✓	✓			✓	✓	Jordan	EnergyPLAN
Alsheghri A et al. /2015 [14]	✓	✓				✓		Dubai, UAE	RET Screen
Wu et al./2018 [13]		✓		✓	✓	✓	House Load	Khorasan, Iran	Tabu Search
Kabir K et al. /2018 [15]		✓				✓		Sandwip, Bangladesh	HOMER & Toray
Ghenai Helal et al. /2019 [16]	✓/–	✓		✓		✓	Agriculture Farm	Sharjah, UAE	Homer Pro
Mousavi/2021 [17]		✓		✓	✓/–	✓	House Load	Tehran, Iran	Homer Pro
Ajiwiguna T. et al./2022 [12]		✓		✓		✓		Wando Island, South Korea	Spyder-Python
Dawoud M et al./2024 [11]		✓				✓		Egypt	GIS site selection

Table 1 (right). Literature review

Authors/Year	Feature
Novosel et al./2015 [10]	Increased the share of intermittent renewables in the production of electricity up to 76% Reduction of CO_2 emissions and costs
Alsheghri A et al. /2015 [14]	Produced water = 0.225 \$/m^3. Reduce the emission of GHG by 1035 CO_2 84% reduced water production subsidies
Wu et al./2018 [13]	NPC: 28,130 USD Produced water: 1.59 to 2.39 USD/m^3 COE: 0.3975 to 0.5975 USD/kWh
Kabir K et al. /2018 [15]	Produced water = 0.002\$/litre system electricity cost = 0.13\$/kWh
Ghenai Helal et al. /2019 [16]	Grid-connected PV COE: (85\$/MWh), Renewable fraction (67%), Greenhouse gas emissions (208 kg/MWh)
Mousavi/2021 [17]	With out DG: NPC: \$10,245, COE: 0.31 \$/kWh GHG emission-free CC dispatch strategy
Ajiwiguna T. et al./2022 [12]	Adding seasonal water storage tank The water production cost declined from 10.21 to 2.31 USD/m^3 and from 36.96 to 3.06 USD/m^3 for constant and variable demand
Dawoud M et al./2024 [11]	Cost of desalination = 0.55–0.63 USD/m^3 Capital expenditure of capacity =760–850 USD/m^3

2. Drinking water quality standards

Water contamination standards rely on toxicological research findings that identify health risks. Health Canada [18], The World Health Organization (WHO) [19], and the United States Environmental Protection Agency (EPA) [20] provide drinking water guidelines. In Newfoundland and Labrador, Health Canada's standards are used. Table 2 compares the three mentioned guidelines.

Table 2. Drinking water quality guidelines (in mg/L unless otherwise stated) [18, 19, 20]

Compound	Health Canada (2022)	WHO (2022)	US EPA (2024)
Microbiological Parameters			
Escherichia coli (*E. coli*)	Nondetectable per 100 mL	Nondetectable per 100 mL	
Chemical and Physical Parameters			
Aluminum	2.9	0.2	NA
Arsenic	0.01 ALARA	0.01	0.01
Chromium	0.05	0.05	0.1
Copper	2	2	1.3
Fluoride	1.5	1.5	4
Manganese	0.12	0.5	0.05
Mercury	0.001	0.001	0.002
Nitrite	3 as nitrite; 1 as nitrite nitrogen	3	1.0
Haloacetic acids—Total (HAAs)	0.08	NA	0.060
Iron	AO: ≤0.3	NA	NA
Lead	0.005 ALARA	0.01	0.015
Colour	15 TCU	15 TCU	15 TCU
pH	7.0–10.5	6.5–8.5	6.5–8.5
Sulphate	AO: ≤500	NA	250
Total dissolved solids (TDS)	AO: ≤500	NA	500
Bromodichloromethane	0.016	0.060	0.08
Trihalomethanes3 (THMs)	0.1	0.1	0.08

2.1 *Water desalination*

The technology employed for water desalination can be broadly classified into two categories—thermal and membrane-based processes. Thermal desalination comes in various types: multi-stage flash distillation (MSF), multi-effect distillation (MED), and mechanical or thermal vapor compression (MVC) or (TVC). These methods rely on the use of heat and electricity for operation. Heat is utilized to elevate the temperature of the saline feed, while electricity powers the relevant pumps. When it comes to desalination via membrane technologies, RO and electrodialysis (ED) are the methods predominantly employed [21]. On the other hand, electricity is solely necessary for RO for the purpose of water pumping and for ion separation between electrodes in ED [22].

Fossil fuels affect the environment adversely because of greenhouse gas emissions if they are used to supply power for the water desalination process. Emissions resulting from the desalination process are predicted to reach billion tons of CO_2 equivalents per year by 2050 [23]. However, dependency on fossil fuels to supply the required energy for desalination can affect the economic side of the process due to fossil fuel price fluctuations [24].

Thermal desalination technologies are less attractive compared to RO due to their higher energy requirements and maintenance costs [25]. Therefore, in many projects all over the world, thermal desalination technologies are being substituted by membrane-based technologies because of their lower energy demand [26].

2.2 *RO systems*

The fundamental principle of osmosis is the migration of water molecules from a solution of lower concentration to one of higher concentration through a semi-permeable membrane. This movement leads to the dilution of the highly concentrated solution until a state of equilibrium is achieved [27]. One of the primary benefits of desalting sea or brackish water using RO membrane technology is the elimination of low molecular solutes. The density of these membranes necessitates the application of considerable pressure to facilitate the passage of water through them. To accomplish this, the applied pressure must exceed the osmotic threshold, which is typically between 25 and 30 bar at 25 °C [28].

RO system mainly consists of 4 stages:

(i) Pretreatment techniques such as flocculation, chemical treatment, sand filtration, and micro cartridge filters not only enhance the productive lifespan of membranes but also diminish the utilization of chemicals, thereby reducing cleaning costs. (ii) A high-pressure pump is employed to create the necessary pressure differential to facilitate the movement of water across the membrane. (iii) A modular treatment involving the use of reverse osmosis technology under the effect of pressure enables the separation of fresh water from the concentrated feed water. (iv) The post-treatment process involves

remineralization and disinfection of the water for the purpose of drinking water distribution. The injection of lime to adjust the pH level clarifies the water [29]. Figure 1 indicates a diagram of an RO desalination system.

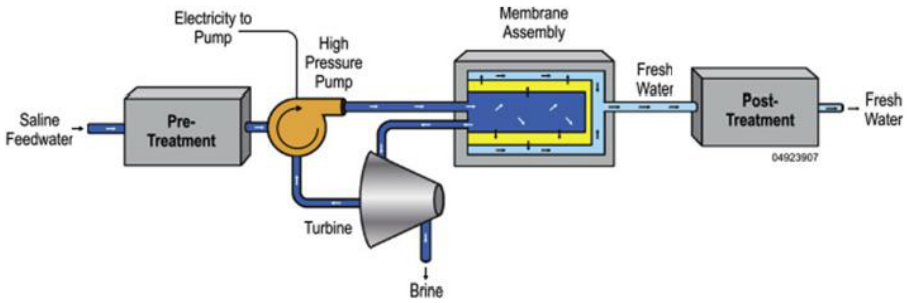

Figure 1. Schematic diagram of RO system [21]

3. Identification of a site

McCallum, with a total population of 45, is located on the southern coast of Newfoundland Island. Its accessibility is restricted to air or sea transport. It's nestled between two hills and sits in a secluded harbor, as seen in Figure 2. McCallum was chosen for investigation due to water-related issues, including scarcity and quality and its lack of connection to the grid.

Figure 2. Selected site McCallum, newfoundland and labrador

3.1 *Water scarcity*

According to The Canadian Drought Monitor (CDM)—Canada's authoritative body for drought monitoring and reporting, McCallum is currently experiencing abnormally dry conditions [30]. Furthermore, due to water scarcity, residents in McCallum collect rainwater as a solution for water management.

3.2 *Water quality issue*

The water supply in McCallum, Newfoundland and Labrador, has been contaminated with lead since 2019. Recent samples from 2022 and 2023 revealed lead concentrations of 0.02 mg/L and 0.016 mg/L, respectively [31]. These levels significantly exceed the maximum allowable limit for lead in drinking water, which is 0.005 mg/L. WHO identifies lead as a major health concern [32]. Even minimal lead exposure in children can impact intellectual development and cause anemia. Pregnant women exposed to lead may experience premature births, smaller babies, reduced mental abilities, and learning difficulties [33]. The neurological system is especially susceptible to lead exposure [34]. Additionally, early childhood exposure to lead has been linked to decreased IQ in later years [35]. Evidence shows lead presence in the water in much of the province [36]. Lead can also enter drinking water from lead service lines and lead-containing plumbing, particularly in the presence of corrosive water [37].

3.3 *Electricity source*

Remote communities like McCallum rely on diesel generators for electricity due to the high cost of connecting to an interconnected grid [38]. These isolated communities face expensive electricity generation expenses due to fuel and maintenance costs. To alleviate this burden, approximately 75% of the cost is subsidized by others connected to the transmission grid, ensuring fair and affordable access to electricity for all [39].

The RO system can purify toxic heavy metals such as lead (Pb) over 99%, even in relatively low pressure [40]. Given the lead contamination at this site, RO is the most suitable desalination method, ensuring safe and clean drinking water. Additionally, RO systems have lower energy requirements and maintenance costs compared to thermal desalination technologies.

3.4 *Electric load demand*

On average, Canadians use approximately 223 litres of water per person per day—making Canada one of the largest per capita water consumers in the world [41]. Currently, 45 individuals reside in MacCallum [42]. The primary water source for this locality is a well, the depth of which measures 16.8 m [43]. Given the population's average daily water consumption of 223 liters, the daily demand considering 20% extra capacity would be 3000GPD. No water storage tank can be used at the site due to water freezing issues for 4–5 months of the year. Therefore, the Ro system operates 24/7 and supplies water, ensuring that running water does not freeze in the pipes and provides water for all houses. The RO system is designed as an isolated system because the community's diesel plant does not run continuously and is low in reliability. To get water from the well the total dynamic head of 100 m and a rated flow rate of about 2.5 GPM, a 1 phase 60 Hz stainless steel pump with a 0.5 hp submersible pump [44] working 24 h is used based on its total dynamic head and flow curve pump. To produce 3000 GPD fresh water for the community, the RO system with a capacity of 3000 GPD and a power consumption of 0.75 hp [44], operating 24 h, is selected [45]. This means the 1.25 hp, equivalent to 0.93 kW, load is distributed evenly throughout the day. Therefore, the proposed HES system should supply an average of 22.37 kWh per day with a peak power of 1.71 kW. The load Profile is shown in Figure 3. The load profile is constructed by calculating the total energy consumption required to operate the RO system and the pump continuously over a 24-h period. Since both systems operate 24/7, the load remains constant throughout the day. This assumption is made to ensure a steady supply of water and to prevent freezing in the pipes, which could occur if the water flow were intermittent.

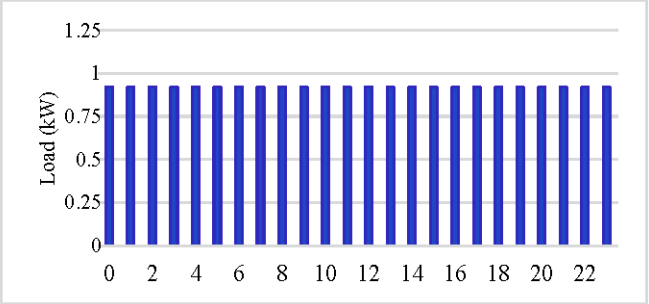

Figure 3. Load profile

The schematic of the system's load includes a submersible pump, a high-pressure pump, and a Ro system, as depicted in Figure 4.

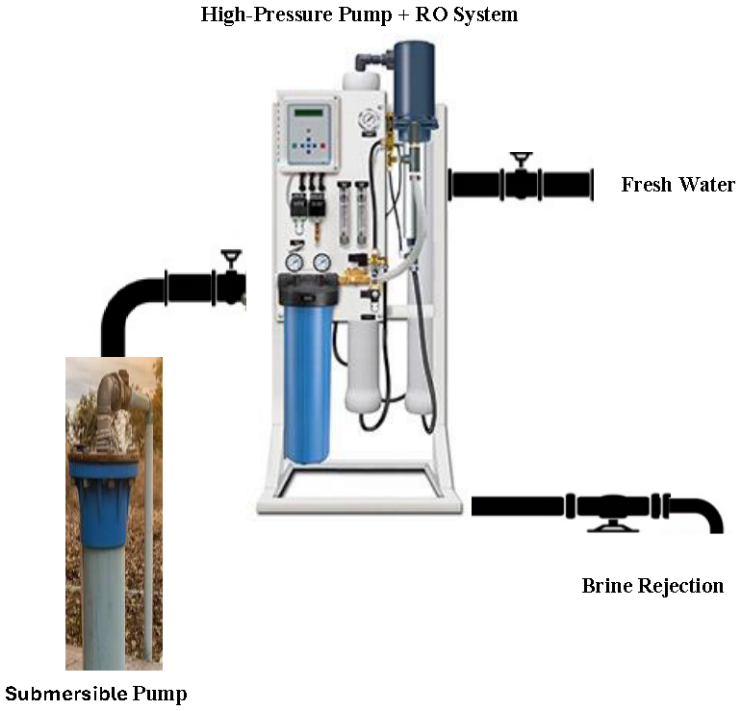

Figure 4. Water system configuration

4. Sources of renewable energies

In this study, the meteorological data related to solar radiation, wind speed, and temperature have been acquired from the NASA Prediction of Worldwide Energy Resource (POWER) database for McCallum, considering a Latitude of 47.6311 and a Longitude of −56.2292.

4.1 *Solar potential assessment*

The Global Horizontal Irradiance (GHI) and related clearness index are indicated in Figure 5. Between May and July, the site receives the highest solar irradiation (over 5 kWh/m^2/day), while December has the lowest radiation. NASA estimates an annual average GHI of 3.17 kWh/m^2/day for the site.

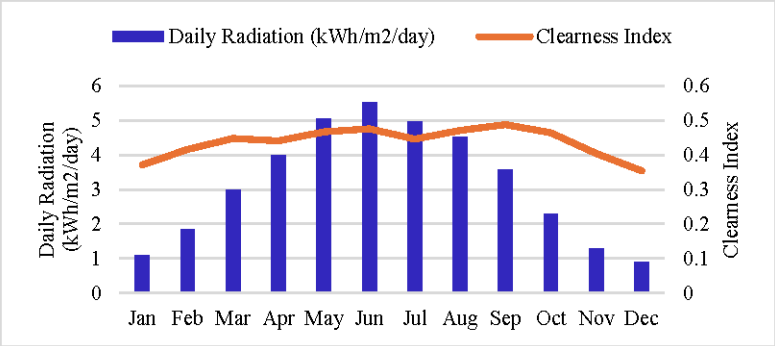

Figure 5. Average daily radiation and clearness index data

4.2 *Wind and temperature assessment*

Figure 6 shows NASA's website data regarding monthly mean wind speed and temperature. The daily average wind speed is 5.9 m/s at an elevation of 50 m. The temperature will also be recorded due to its effect on both solar PV and wind turbine efficiency. The scaled Annual average temperature is 4.41 °C. From December to March, the mean monthly temperature is negative, indicating the cold climate of the selected site.

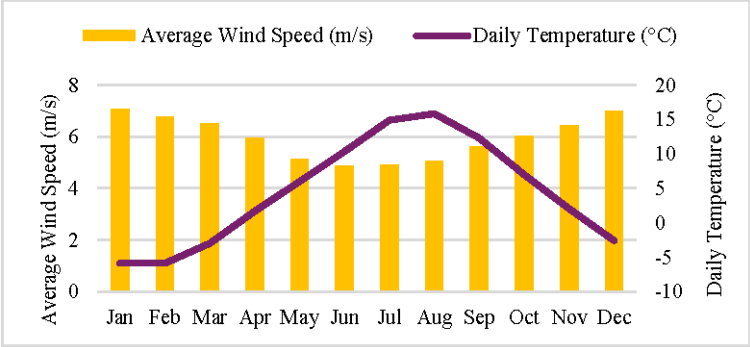

Figure 6. Average wind speed and daily temperature data

5. Methodology and configuration of system

In this study, we propose an HES to enhance reliability, meet energy demand, and reduce reliance on solar and wind energy variations. The HES comprises five key components: PV modules, a wind turbine, a converter, batteries, and a diesel generator. Using Homer Pro software, developed by the National Renewable Energy Laboratory (NREL), assists engineers by facilitating the optimization and selection of viable solutions from technical, economic, and environmental perspectives [46]. Here, we determined the optimal HES configuration based on cost-effectiveness throughout its life cycle. Figure 7 illustrates the system configuration, and Table 3 reveals the estimated costs for each component.

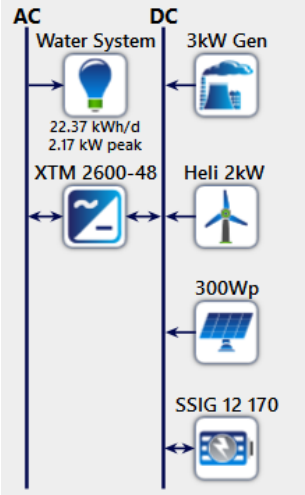

Figure 7. Schematic diagram of HES system

Table 3. Capacity and costs of components

Components	Capacity	Initial Cost	Replacement Cost	O&M Cost
PV Panel	0.300 kW	$500	$400	$5 /year
Wind Turbine	2 kW	$6000	$4500	$20/year
Battery	12 V 170 Ah	$446	$446	–
Converter	2.6 kW	$4000	$4000	–
Diesel generator	3 kW	$1350	$1350	$0. 3/op. hour

5.1 *PV modules*

The chosen *PV* module is a 72-cell Panasonic Mono crystalline with an *STC* power rating of 300 watts and 15.17% efficiency. This module's high snow and wind load rating feature makes it a good option for the selected site. The expenses of capital and replacement are $500 and $400 per panel, respectively [47]. The higher cost is due to the site's remote location. Operating and maintenance (O&M) cost is $5 yearly. *PV* system can generate output power, which can be calculated using Equation (1) [48]:

$$P_{PV} = Y_{PV} f_{PV} \left(\frac{G_T}{G_{T,STC}} \right) [1 + \alpha_P (T_c - 25)] \tag{1}$$

where Y_{PV} represents the *PV* rated power (kW) under standard test conditions (*STC*), α_p shows the power coefficient related to temperature (%/ °C), and f_{PV} is the de-rating factor of *PV* (%), $G_{T,STC}$ is radiation under *STC* (kW/m^2), G_T is the actual solar radiation of the *PV* panel (kW/m^2). It should be noted that T_c is the *PV* cell's temperature (°C), whereas Figure 6 shows ambient temperature (T_a). The relationship between T_c and T_a is shown in Equation (2) [49].

$$T_c = T_a + \left(\frac{G_T}{800} \right) \times [NOCT - 20] \tag{2}$$

where T_a is the ambient temperature, G_T is the solar radiation intensity on the *PV* module surface, and *NOCT* is the nominal operating temperature of the *PV* cell, which is provided in the datasheet of the *PV* module.

5.2 *Wind turbine (WT)*

An upwind 3-bladed WT with 18 m hub height and rated power of 2 kW with an output voltage of 48 V DC was used in this design. The capital and replacement costs for each WT were considered $6000 and $4500 [50], respectively, and the related O&M cost was $20 per year. Lifetime is 20 years, and based on the datasheet, at the average wind speed of our site (5.9 m/s), about 6200 kWh of energy can be acquired yearly. The power curve for this WT is shown in Figure 8.

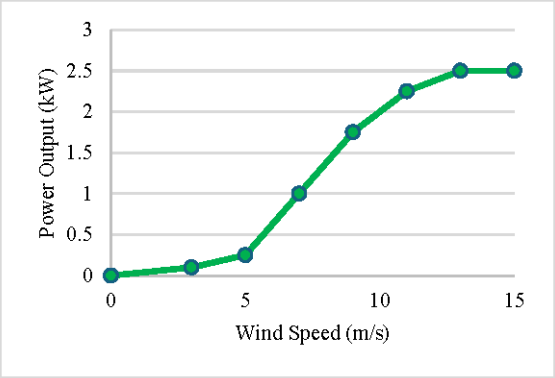

Figure 8. Wind turbine power curve

Actual wind turbine output power can be determined by applying Equation (3) [51]:

$$P_{WTG} = \left(\frac{\rho}{\rho_0}\right) P_{WTG,STC} \tag{3}$$

where, $P_{WTG,STC}$ refers to the output power of the wind turbine in *STC* condition, and ρ and ρ_0 = 1.225 kg/m^3 are, respectively, air densities in actual and *STC* conditions.

5.3 *Converter*

The converter is used to provide a flow of electricity between components of DC and AC buses. Ten years of lifetime and 96% efficiency is considered for the inverter input; on the other hand, a relative capacity of 100% and 96% efficiency is considered for the rectifier input. The capital and replacement costs, including wiring on the remote location, are considered $4000 for the selected converter [52]. The Required capacity of the converter for the system can be calculated using the formula presented in Equation (4) [45]:

$$C = (3L_i) + L_r \tag{4}$$

where L_i and L_r indicate inductive load and resistive loads, respectively.

5.4 *Diesel generator*

In this paper, a 3 kW DC diesel generator with a 15,000-h lifetime ideal for battery charging is used; the cost of capital is $1350 with O&M cost of $0. 30 each hour. When calculating the total cost of diesel generators, fuel costs, which fluctuate based on global oil prices, have considerable effects. Furthermore, based on the pricing zone provided by NL Public Utilities Board, which considers differences in fuel product prices, including transportation costs, volume of sales, storage costs, distribution costs, and inventory rates. Diesel price is considered $1.86 per liter in McCallum [53]. More details about the generator are provided in Table 4 based on the Homer simulator.

Table 4. Fuel and emission properties of the generator

Fuel	Diesel
Fuel curve intercept (L/hr)	0.144
Fuel curve slope (L/hr/kW)	0.286
Emissions	
CO (g/L fuel)	19.76
Unburned HC (g/L fuel)	0.72
Particulates (g/L fuel)	1.198
Fuel Sulfur to PM (%)	2.2
NOx (g/L fuel)	22.46
Fuel Properties	
Lower Heating Value (MJ/kg)	43.2
Density (kg/m^3)	820
Carbon Content (%)	88
Sulfur Content (%)	0.4

We can refer to Equation (5) to find the rate of consumed fuel F_d by generator per hour (L/h):

$$F_d = aT_d + bP_{rated} \tag{5}$$

where T_d and P_{rated} are actual power and rated power of the generator, a and b are the coefficient of fuel curve intercept and curve slope. As a result, the cost of consumed fuel per hour can be calculated by Equation (6):

$$C_f = F_d \times F_p \tag{6}$$

where F_p refers to price of fuel [54].

5.5 *Battery*

To store excess energy produced by the hybrid system and supply power during shortages, a string of four series-connected 12 V-170 Ah Trojan SSIG batteries with 80% efficiency is used [55]. These batteries create a 48-volt DC bus voltage compatible with the selected converter. We increase the number of parallel strings as needed based on optimization to add backup time. The cost for each battery is $446. Capacity for each battery is given by Equation (7).

$$C_{Bat} = \frac{AD \times E_L}{\eta_{Inv} \times \eta_{Bat} \times DOD} \tag{7}$$

where E_L is the average daily load demand (kWh/day), AD refers to autonomous days, DOD is battery depth of charge, η_{Inv} and η_{Bat} are efficiencies related to inverter and battery.

5.6 *Economic analysis*

The main criteria for ranking the optimal system in Homer Pro is based on comparing NPC and COF for different configurations of the system during its lifespan. NPC calculation is done using Equations (8) and (9) [56]:

$$NPC = \frac{C_{annual,total}}{CRF(r,N)} \tag{8}$$

$$CRF(r,N) = \frac{r(1+r)^N}{(1+r)^N - 1} \tag{9}$$

where $C_{annual,total}$ is the total cost per year ($/yr) and $CRF(r,N)$ refers to the capital recovery factor which is a function of the annual real interest rate (r) and the total project lifespan (N). In Homer Pro, the annual real interest rate (r) is calculated internally by inserting the discount rate or the rate of borrowing money (i) and inflation rate (f) using Equation (10) [57]:

$$r = \frac{i-f}{1+f} \tag{10}$$

In the proposed system N, i and f in Homer are considered 25, 8.25% [57], 2.8% [58].

COE is the average cost of electricity kWh over a selected currency. The Equation (11) is used for calculation [59]:

$$COE = \frac{C_{annual,total}}{E_{GYS}} \tag{11}$$

where E_{GYS} refers to the total load (kWh) that is served yearly.

The salvage cost represents the estimated resale value of system components after the project's lifespan. It plays a crucial role in calculating the NPC, and the equation (12) is for determining it [60].

$$SC = C_R \frac{T_{rem}}{T_{com}} \tag{12}$$

where CR is the replacement cost ($), T_{rem} is the years the component can be used, and T_{com} is the expected years of lifetime for the component (year).

5.7 *Dispatch strategies*

Based on selected sources of power and the potential of resources in the selected site, the optimization method adopts different dispatch strategies. When renewable energy isn't enough to meet the demand, a dispatch strategy consists of guidelines that dictate how generators and energy storage systems should operate. These rules help manage the available resources effectively [61].

In this study, two dispatch strategies are used: load following (LF) and cycle charging (CC). In the LF strategy, when renewable energy falls short of meeting the load demand, the diesel generator first steps in to meet the primary load requirements. The renewable energy source then focuses on charging the battery. In contrast, under the CC strategy, the diesel generator handles both the primary load supply and battery charging. However, this approach results in higher gas emissions than the LF strategy [62]. The energy storage system in CC is the main component, as it is continuously charged using any available excess power [63].

6. Results and discussion

Homer Pro uses advanced optimization algorithms to find the best combination of components that meet the load demand at the lowest cost. Furthermore, it incorporates several features to ensure that the power balance constraint can be met even under worst-case scenarios. These features include sensitivity analysis and scenario analysis, which allow users to explore how variations in key parameters, such as renewable energy availability and load demand, affect system performance. The configuration optimization is solved considering:

- **Objective Function:** The primary objective is to minimize the NPC of the HES considering current economic parameters such as discount rate and inflation rate in project lifespan while ensuring reliable electricity supply for the RO system.
- **Decision Variables:** Capacities of each component.

- **Main Constraints:** The total energy generated must meet the energy demand of the RO system.
  - **Capacity Constraints:** Each component's capacity must be within feasible limits.
    - **Maximum PV Capacity:** The load is 22.37 kWh/m^2/day. The efficiency of the PV module is 15.17%, with a coefficient factor for the stationary PV system of 0.7 and irradiance of 3.17 kWh/m^2/day. The required area for the system is a maximum of 66 m^2. Considering a 300-watt PV module, each with an area of 1.456 m^2, the maximum PV capacity would be approximately 13.5 kW.
    - **Maximum Wind Turbine Capacity:** 2 kW.
    - **Maximum Diesel Generator Capacity:** 3 kW.

Here, we have identified six different configurations that represent the most optimized options, considering all input constraints to meet the required load demand. Table 5 provides detailed specifications, and Figure 9 compares the NPC and COE for each system. Techniques like the Analytic Hierarchy Process (AHP) should be applied to rank all proposed configurations. AHP will be used to evaluate and rank the configurations based on criteria such as cost, reliability, environmental impact, and renewable fraction. The goal is to determine the best HES configuration for RO systems. Let's delve into these configurations:

Case I (PV/WT/generator/battery): This configuration excels in economic terms while maintaining the highest reliability. It boasts a high renewable fraction, and it produces 29% of extra electricity.

Case II (PV/WT/battery): Both PV and wind contribute to this system, resulting in a 100% renewable fraction. Therefore, no fuel usage leads to zero gas emissions.

Case III (WT/generator/battery): A combination of wind and generator, with approximately 25% of the load demand supplied by the generator.

Case IV (PV/generator/battery): Here, the load is primarily supplied by the PV system, achieving about a 96% renewable fraction. The generator plays a supporting role.

Case V (PV/battery): 100% renewable fraction system, with no fuel usage but the longest hour of autonomy.

Case VI (generator): Despite having the least initial capital, this option has zero renewable fraction and the highest NPC. This case is the worst option, considering reliability and environmental emissions.

Table 5. Homer simulation results for different scenarios

Parameters	Case I	Case II	Case III	Case IV	Case V	Case VI
PV (kW)	3.19	4.11		9.13	13.5	
Wind (kW)	2	2	2			
Generator (kW)	3		3	3		3
Converter (kW)	1.56	1.59	1.58	1.56	1.58	1.56
Battery (Qty)	16	24	24	20	28	
Dispatch Strategy	LF	CC	CC	LF	CC	CC
Total NPC	$44,382	$45,259	$64,176	$65,829	$69,392	$153,940
COE ($/kWh)	$0.397	$0.405	$0.575	$0.590	$0.621	$1.380
Unmet electric load (kWh/year)	0.71	1.1	0.429	0.692	0.772	0.612
Capacity shortage (kWh/year)	7.86	7.88	6.05	7.75	6.87	7.22
Excess electricity (%)	29	36	3.66	37.2	56.3	1.77
Renewable fraction (%)	98.8	100	73.8	95.6	100	0
Autonomy (hr)	27.7	41.6	41.6	34.6	48.5	0
Fuel (L/yr)	45.9	0	717	161	0	3738

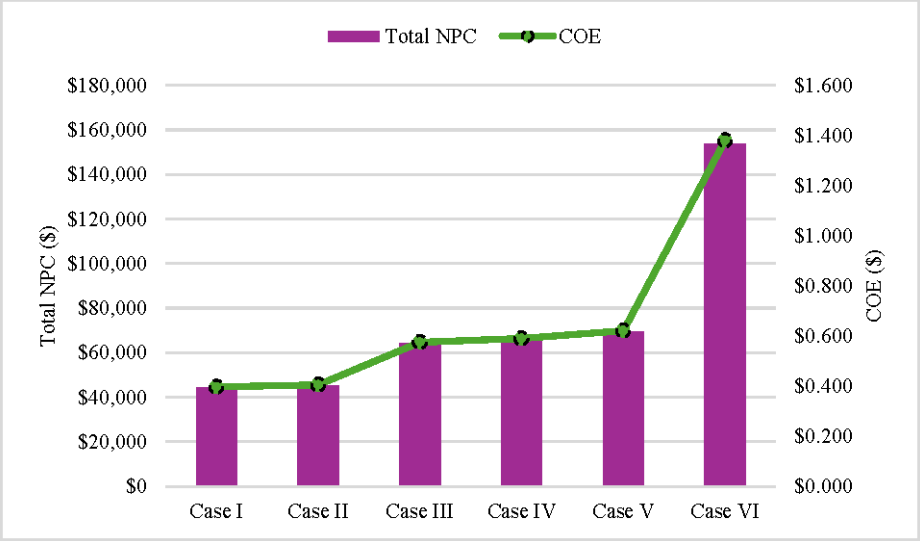

Figure 9. NPC and COE for different scenarios

Figure 10 shows the yearly total electricity production and each system's component share. Total AC load is 8164 kWh/year; therefore, production more than this amount would be considered excess energy. The amount of excess energy in each scenario is shown in Figure 10.

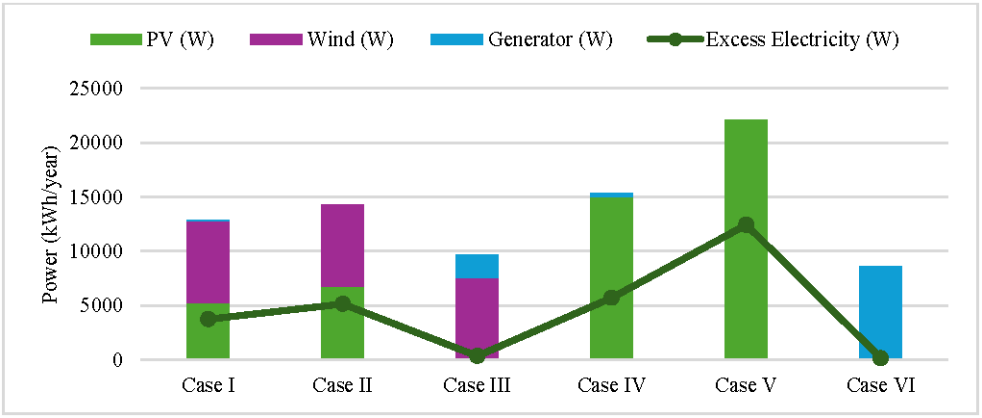

Figure 10. Total yearly electricity production for different scenarios

6.1 *Optimized system*

The optimized system can help the community access a reliable and less fossil fuel-based power system configuration. In Case I, the amount of produced electricity by PV modules and wind turbine can't meet the load demand; therefore, based on the adopted dispatch strategy, LF, a comparison between two costs, battery discharge and running of the generator, is done, and least cost which is a combination of generator and battery is chosen. In other words, in this configuration, to fully account for the uncertainty of renewable power, the diesel generator serves as a backup power source and charges the battery when the RESs and/or the storage system cannot meet the load's energy demand.

Here, the NPC of the optimized system is shown in Figure 11 different expenses are illustrated based on each system's element share.

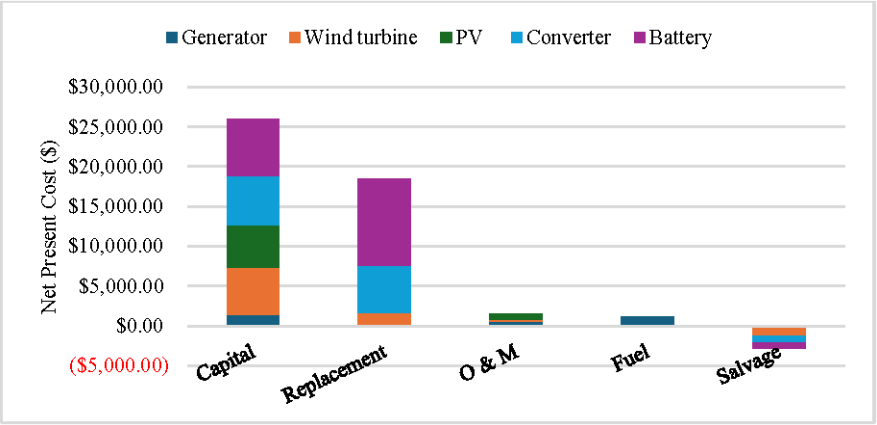

Figure 11. NPC details for the optimized hybrid system

The overall capital cost is $26,031, with the most significant share for the battery accounting for $7136 or 27% of total initial cost, followed by the converter with $6223 or 24% share. The total replacement cost is $18,482, which is also mainly related to the storage system and converter. There is no replacement cost for PV and generator because the lifetime for the mentioned components is considered as long as the project lifetime. The estimated O&M, Fuel, and salvage costs for the proposed system are $1510, $1167, and $−2807, respectively.

As indicated in Figure 12, the generator generally operates between 12 AM and 10 AM, when lower sun irradiance is available, and the generator runs to recharge the batteries.

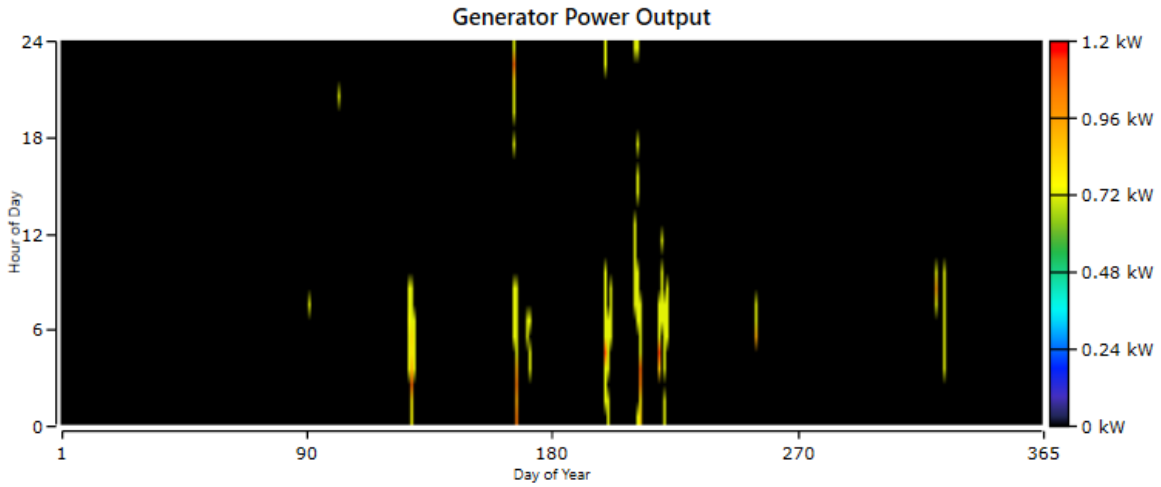

Figure 12. Hourly and monthly generator power output

State of the charge (SOC) in the storage system is mainly in good condition, higher than 84 percent, as illustrated in Figure 13 in May, June, and July, minimum charging cycles occurred, which are due to less output power in WT and PV panels caused by reduction of wind and irradiation resources. This can also be seen in Figure 12, where peak power in the generator mainly happened in the same periods as a backup source of power.

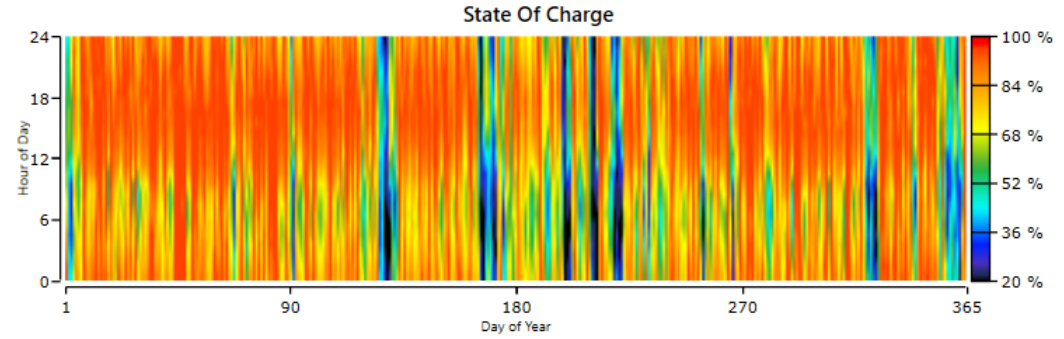

Figure 13. Hourly and monthly battey state of the charge

Figure 14 shows that AC load is mainly met by renewable energy in the time series results from HOMER Pro; it signifies an optimal system configuration and resilience since it ensures uninterrupted power supply even during extended periods of renewable resource availability (e.g., cloudy days or calm winds). The battery storage and the generator as backups play crucial roles in maintaining this balance during low-resource periods.

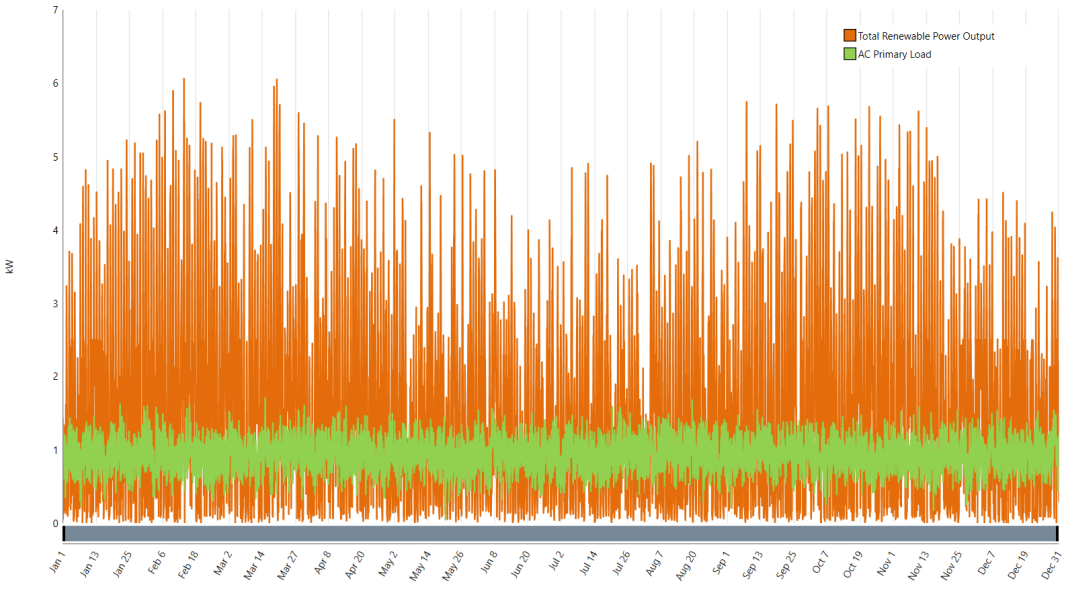

Figure 14. Time series result for total renewable power output and AC primary load

6.2 *Sensitivity analysis*

In this section, sensitivity analyses were conducted to explore how changes in specific variables can affect the off-grid system's behaviours and ability to meet the load requirements.

6.2.1 *Fuel price*

Diesel prices are subject to global exchange rate fluctuations. However, remote areas often face higher and more variable diesel costs due to transportation expenses and other associated factors. To assess its impact, diesel price range of $1.66/L to $2.16/L in Canada that happened from 2022 to 2024 [64] was assumed. As the fuel price increases from $1.66/L to $2.16/L, both NPC and COE increase, as shown in Figure 15; simultaneously, fuel consumption decreases from about

58 L/yr to 30 L/yr. This variation occurs because the hybrid system increasingly relies on renewable energy components, reducing generator operation hours and resulting in higher renewable fraction and consequently lower CO_2 emissions but higher NPC and COE.

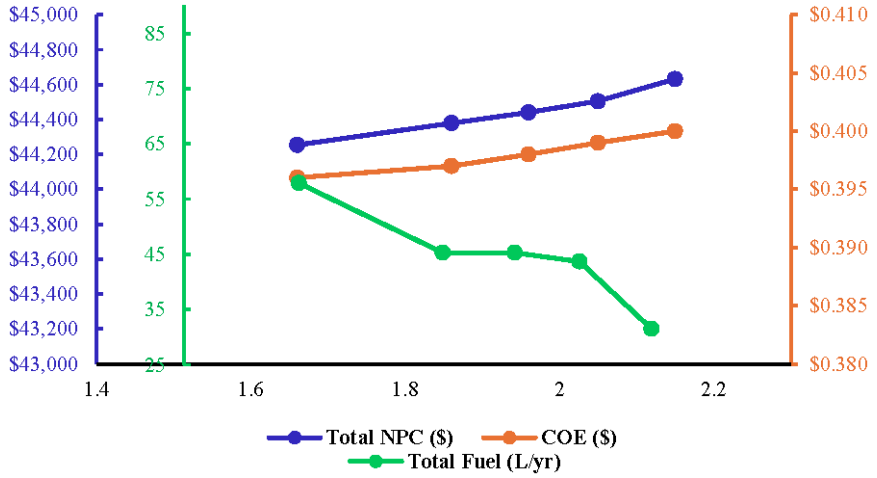

Figure 15. Sensitivity analysis for different fuel prices

6.2.2 *Annual average load*

Over time, it may be necessary to increase the load due to rising demand resulting from population growth. This increase would affect the annual average load. To simulate this situation, we consider sensitivity for the scaled annual average kWh/day. Evaluating the results, we increased the load from 22.37 to 25.4 kWh/day. This can be seen in Figure 16. As the load increases, both NPC and COE rise. At the minimum load of 22.37 kWh/day, the NPC is $44,382, the COE is 0.397/kWh, and excess energy is 29%. However, when the load is increased to 25.4 kWh/day, the NPC and COE reach $50,912 and $0.402, respectively, while excess energy decreases by approximately 25%. It's important to note that beyond 26 kWh/day, the optimized configuration, including the number of batteries, changes, making further comparison impossible.

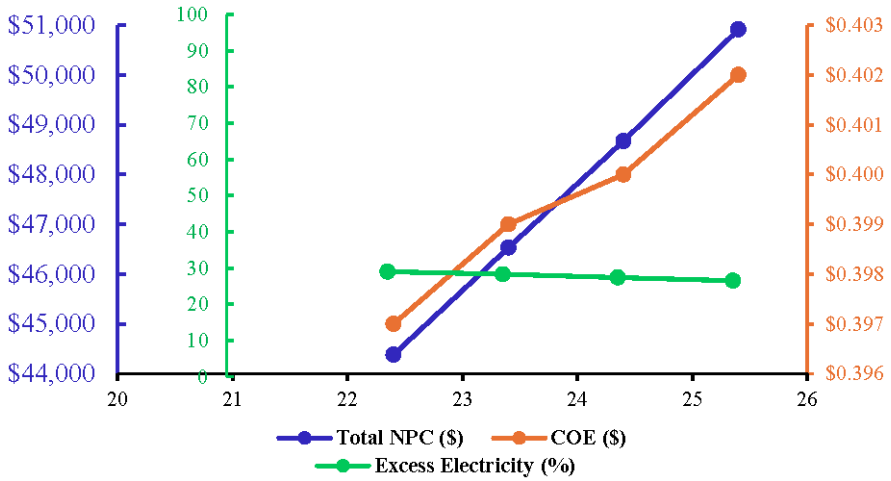

Figure 16. Sensitivity analysis for different annual average loads

7. Conclusions

The result acquired from Homer Pro software indicates that the proposed system, consisting of PV panels, a wind turbine, a generator, and a battery, is the most cost-effective option. The electricity for the community water system, including a submersible pump and an RO system, is fully supplied by renewable energy, including the wind turbine and PV panels. In case of inadequate wind and solar resources, the battery system and diesel generator operate as backup systems. The system is highly reliable and has LF dispatch strategy. The sensitivity analysis conducted in Homer reveals that when diesel fuel prices rise, generator operation hours decrease, leading to reduced fuel consumption and a shift toward a higher renewable energy fraction. Additionally, as the annual average load increases while maintaining the same configuration, excess energy diminishes due to population-driven demand. In both scenarios, the NPC and COE increase.

Conflict of interest

There is no conflict of interest for this study

References

[1] U.S. Geological Survey, "Where is Earth's Water?" Accessed: May 18, 2024. [Online]. Available: https://www.usgs.gov/special-topics/water-science-school/science/where-earths-water.

[2] United Nations, "The United Nations World Water Development Report 2015: Water for a Sustainable World," Accessed: Aug. 31, 2024. [online]. Available: https://www.unwater.org/publications/un-world-water-development-report-2015.

[3] K. Elsaid, M. Kamil, E. T. Sayed, M. A. Abdelkareem, T. Wilberforce, and A. Olabi, "Environmental impact of desalination technologies: A review," *Sci. Total Environ.*, vol. 748, p. 141528, 2020.

[4] E. Jones, M. Qadir, M. T. H. van Vliet, V. Smakhtin, and S. Kang, "The state of desalination and brine production: A global outlook," *Sci. Total Environ.*, vol. 657, pp. 1343–1356, 2019.

[5] D. S. Ayou, H. M. Ega, and A. Coronas, "A feasibility study of a small-scale photovoltaic-powered reverse osmosis desalination plant for potable water and salt production in Madura Island: A techno-economic evaluation," *Therm. Sci. Eng. Prog.*, vol. 35, p. 101450, 2022.

[6] J. Wang, S. L. Li, Y. Guan, C. Zhu, G. Gong, and Y. Hu, "Novel RO membranes fabricated by grafting sulfonamide group: Improving water permeability, fouling resistance and chlorine resistant performance," *J. Membr. Sci.*, vol. 641, p. 119919, 2022.

[7] A. Panagopoulos, K. J. Haralambous, and M. Loizidou, "Desalination brine disposal methods and treatment technologies—A review," *Sci. Total Environ.*, vol. 693, p. 133545, 2019.

[8] G. D. Pimentel da Silva and M. H. Sharqawy, "Techno-economic analysis of low impact solar brackish water desalination system in the Brazilian Semiarid region," *J. Clean. Prod.*, vol. 248, p. 119255, 2020.

[9] S. Koohi-Fayegh and M. A. Rosen, "A review of energy storage types, applications and recent developments," *J. Energy Storage*, vol. 27, p. 101047, 2020.

[10] T. Novosel, B. Ćosić, T. Pukšec, G. Krajačić, N. Duić, and B. V. Mathiesen, "Integration of renewables and reverse osmosis desalination—Case study for the Jordanian energy system with a high share of wind and photovoltaics," *Energy*, vol. 92, no. Part 3, pp. 270–278, 2014.

[11] M. A. Dawoud, G. R. Sallam, M. A. Abdelrahman, and M. Emam, "The Performance and Feasibility of Solar-Powered Desalination for Brackish Groundwater in Egypt," *Sustainability*, vol. 16, no. 4, p. 1630, 2024.

[12] T. Ajiwiguna, G. R. Lee, B. J. Lim, S. M. Choi, and C. D. Park, "Design strategy and economic analysis on various configurations of stand-alone PV-RO systems," *Desalination*, vol. 526, p. 115547, 2022.

[13] B. Wu, A. Maleki, F. Pourfayaz, and M. A. Rosen, "Optimal design of stand-alone reverse osmosis desalination driven by a photovoltaic and diesel generator hybrid system," *Solar Energy*, vol. 163, pp. 91–103, 2018.

[14] A. Alsheghri, S. A. Sharief, S. Rabbani, and N. Z. Aitzhan, "Design and Cost Analysis of a Solar Photovoltaic Powered Reverse Osmosis Plant for Masdar Institute," *Energy Procedia*, vol. 75, pp. 319–324, 2015.

[15] K. M. Kabir, M. A. Matin, H. Misran, and N. Amin, "A Case Study on Cost-efficient Solar Powered Drinking Water System for Isolated Communities," in *Proc. 2018 Int. Conf. Innovation Eng. Technol. (ICIET)*, Dhaka, Bangladesh, Dec. 27–28, 2018.
[16] C. Ghenai, A. Almasri, J. Alrejjal, and N. Khalil, "Modeling, simulation and performance analysis of solar PV integrated with reverse osmosis water treatment unit for agriculture farming," in *Proc. 2019 8th Int. Conf. Modeling Simul. Appl. Optim. (ICMSAO)*, Manama, Bahrain, Apr. 15–17, 2019.
[17] M. Mousavi and M. Iqbal, "Optimum Sizing of Stand-Alone Hybrid Photovoltaic Systems Equipped with Reverse Osmosis Desalination System for a Rural House in Iran," *Jordan J. Electr. Eng.*, vol. 7, no. 4, pp. 304–322, 2021.
[18] Health Canada, "Guidelines for Canadian Drinking Water Quality Summary Tables," Accessed: May 26, 2024. [Online]. Available: https://www.canada.ca/en/health-canada/services/environmental-workplace-health/reports-publications/water-quality.html.
[19] World Health Organization (WHO), "Fourth edition incorporating the first and second addenda Guidelines for drinking-water quality," Accessed: Aug. 31, 2024. [online]. Available: https://www.who.int/publications/i/item/9789240045064.
[20] U.S. Environmental Protection Agency (EPA), "National Primary Drinking Water Regulations," Accessed: May 26, 2024. [Online]. Available: https://www.epa.gov/ground-water-and-drinking-water/national-primary-drinking-water-regulations#four.
[21] A. Al-Karaghouli and L. L. Kazmerski, "Energy consumption and water production cost of conventional and renewable-energy-powered desalination processes," *Renew. Sustain. Energy Rev.*, vol. 24, pp. 343–356, 2013.
[22] D. Zarzo and D. Prats, "Desalination and energy consumption. What can we expect in the near future?" *Desalination*, vol. 427, pp. 1–9, 2018.
[23] World Bank, "Renewable Energy Desalination: An Emerging Solution to Close the Water Gap in the Middle East and North Africa," Accessed: May 8, 2024. [Online]. Available: www.worldbank.org/mna/watergap.
[24] T. Mezher, H. Fath, Z. Abbas, and A. Khaled, "Techno-economic assessment and environmental impacts of desalination technologies," *Desalination*, vol. 266, no. 1–3, pp. 263–273, 2011.
[25] S. F. Anis, R. Hashaikeh, and N. Hilal, "Reverse osmosis pretreatment technologies and future trends: A comprehensive review," *Desalination*, vol. 452, pp. 159–195, 2019.
[26] V. Gude, N. Nirmalakhandan, and S. Deng, "Renewable and sustainable approaches for desalination," *Renew. Sustain. Energy Rev.*, vol. 14, pp. 2641–2654, 2010.
[27] C. Fritzmann, J. Löwenberg, T. Wintgens, and T. Melin, "State-of-the-art of reverse osmosis desalination," *Desalination*, vol. 216, no. 1–3, pp. 1–76, 2007.
[28] W. R. Bowen and P. M. Williams, "Quantitative predictive modelling of ultrafiltration processes: Colloidal science approaches," *Adv. Colloid Interface Sci.*, vols. 134–135, pp. 3–14, 2007.
[29] D. Zioui, H. Aburideh, Z. Tigrine, S. Hout, M. Abbas, and N. K. Merzouk, "Experimental Study on a Reverse Osmosis Device Coupled with Solar Energy for Water Desalination," in *Proc. 2017 Int. Renew. Sustain. Energy Conf. (IRSEC)*, Tangier, Morocco, Dec. 4–7, 2017.
[30] Canadian Drought Monitor, "Canadian Drought Monitor," Accessed: May 8, 2024. [Online]. Available: https://agriculture.canada.ca/en/agricultural-production/weather/canadian-drought-monitor#drou.
[31] Water Resources Portal, "Report Viewer," Accessed: Jun. 23, 2024. [Online]. Available: https://maps.gov.nl.ca/water/reports/viewreport.aspx?COMMUNITY_NAME=McCallum.
[32] World Health Organization, "Lead poisoning," Accessed: May 8, 2024. [Online]. Available: https://www.who.int/news-room/fact-sheets/detail/lead-poisoning-and-health.
[33] Canada Health Act, "Canada Health Act Annual Report 2011–2012," Accessed: May 8, 2024. [Online]. Available: https://www.canada.ca/en/health-canada/services/health-care-system/reports-publications/canada-health-act-annual-reports/report-2011-12.html.
[34] W. Jedrychowski, F. Perera, J. Jankowski, D. Mrozek-Budzyn, E. Mroz, E. Flak, et al., "Gender specific differences in neurodevelopmental effects of prenatal exposure to very low-lead levels: The prospective cohort study in three-year olds," *Early Hum. Dev.*, vol. 85, no. 8, pp. 503–510, 2009.
[35] D. C. Bellinger, K. M. Stiles, and H. L. Needleman, "Low-level lead exposure, intelligence and academic achievement: A long-term follow-up study," *Pediatrics*, vol. 90, no. 6, pp. 855–861, 1992.
[36] K. Thomson, "Potential Human Health Impacts of Water Contaminants in Newfoundland and Labrador," in *Proc. Int. Conf. Mar. Freshwater Environ., iMFE*, Sheraton hotel in St. John's, Canada, Aug. 6–8, 2014.

[37] P. Levallois, P. Barn, M. Valcke, D. Gauvin, and T. Kosatsky, "Public Health Consequences of Lead in Drinking Water," *Curr. Environ. Health Rep.*, vol. 5, no. 2, pp. 255–262, Jun. 2018.
[38] K. Karanasios and P. Parker, "Recent Developments in Renewable Energy in Remote Aboriginal Communities, Newfoundland and Labrador, Canada," *Papers Can. Econ. Dev.*, vol. 16, pp. 109–118, 2016.
[39] "Review of the Newfoundland and Labrador Electricity System," Newfoundland and Labrador. Accessed: Aug. 31, 2024. [online]. Available: https://policycommons.net/artifacts/1224560/review-of-the-newfoundland-and-labrador-electricity-system/1777636/.
[40] E. M. Villena-Martínez, P. A. Alvizuri-Tintaya, J. Lora-García, J. I. Torregrosa-López, and V. G. Lo-Iacono-Ferreira, "Reverse Osmosis Modeling Study of Lead and Arsenic Removal from Drinking Water in Tarija and La Paz, Bolivia," *Processes*, vol. 10, no. 9, p. 1889, 2022.
[41] Statistics Canada, "World Water Day eh," Accessed: May 13, 2024. [Online]. Available: https://www.statcan.gc.ca/o1/en/plus/5814-world-water-day-eh.
[42] "Profile table, Census Profile, 2021 Census of Population—McCallum, Designated place (DPL), Newfoundland and Labrador," Accessed: Jun. 23, 2024. [Online]. Available: https://www12.statcan.gc.ca/census-recensement/2021/dp-pd/prof/details/page.cfm?Lang=E&SearchText=McCallum&DGUIDlist=2021A0006100126&GENDERlist=1&STATISTIClist=1&HEADERlist=0.
[43] Municipal and Provincial Affairs, "Average Well Depth and Yield by Community," Accessed: May 14, 2024. [Online]. Available: https://www.gov.nl.ca/mpa/well/community/.
[44] Pumpsupermarket.com, "2" Thin Submersible Pump 5.2 GPM—3 Wire—170 ft—110/220V—0.5HP," Accessed: Jun. 15, 2024. [Online]. Available: https://www.pumpsupermarket.com/product/2-thin-submersible-pump-5-2-gpm-3-wire-170-ft-110-220v-0-5hp/.
[45] SWT, "BLS Series, 3000 to 9000 GPD, Commercial RO Systems," Accessed: Jun. 11, 2024. [Online]. Available: https://www.swtwater.com/catalog/1298_bls3000.htm.
[46] M. A. Omar, "The Significance of Considering Battery Service-Lifetime for Correctly Sizing Hybrid PV-Diesel Energy Systems," *Energies*, vol. 17, no. 1, p. 103, 2024.
[47] Arntjen Clean Energy Solutions, "Panasonic Solar Panel (Module), 300 Wp, 72-cell, Black on Black," Accessed: Jun. 2, 2024. [Online]. Available: https://store.arntjencleanenergy.com/products/panasonic-solar-panel-module-300w-72-cell-black-on-black?pr_prod_strat=e5_desc&pr_rec_id=c27738c3b&pr_rec_pid=6854361841815&pr_ref_pid=5510759645335&pr_seq=uniform.
[48] N. E. Benti, Y. S. Mekonnen, A. A. Asfaw, M. D. Lerra, T. A. Woldegiyorgis, C. A. Gaffe, et al., "Techno-economic analysis of solar energy system for electrification of rural school in Southern Ethiopia," *Cogent Eng.*, vol. 9, no. 1, p.2021838, 2022.
[49] M. A. Omar and M. M. Mahmoud, "Temperature impacts on the performance parameters of grid-connected PV systems based on field measurements in Palestine," *IET Renew. Power Gener.*, vol. 13, no. 14, pp. 2541–2548, 2019.
[50] "3 kW Small Wind Turbine|Renewable On-Grid & Off-Grid Energy Systems," Accessed: Jun. 17, 2024. [Online]. Available: https://www.ryse.energy/3kw-wind-turbines/.
[51] "How HOMER Calculates Wind Turbine Power Output," Accessed: Jun. 2, 2024. [Online]. Available: https://homerenergy.com/products/front/docs/1.0/how_homer_calculates_wind_turbine_power_output.html.
[52] "Inverter charger multiconnection 2000 W 48 V Studer XTM 2600-48," Accessed: Jun. 18, 2024. [Online]. Available: https://tienda-solar.es/en/off-grid-inverter/111-charger-inverter-multiconnection-2000w-48v-studer-xtm-2600-48.
[53] "Board of Commissioners of Public Utilities," Accessed: Jun. 17, 2024. [Online]. Available: http://www.pub.nl.ca/PP_petroleumproducts.php.
[54] A. Maleki and A. Askarzadeh, "Optimal sizing of a PV/wind/diesel system with battery storage for electrification to an off-grid remote region: A case study of Rafsanjan, Iran," *Sustain. Energy Technol. Assess.*, vol. 7, pp. 147–153, 2014.
[55] "Trojan SSIG 12 170 12V 170Ah Solar Signature Line—Deep Cycle Flooded Batteries—1200 Cycles @ 50% DOD," Accessed: Jun. 2, 2024. [Online]. Available: https://canadianbatterystore.ca/product/trojan-ssig-12-170-solar-signature-line-deep-cycle-flooded-batteries-1200-cycles-50-dod/.
[56] K. Y. Lau, C. W. Tan, and A. H. M. Yatim, "Effects of ambient temperatures, tilt angles, and orientations on hybrid photovoltaic/diesel systems under equatorial climates," *Renew. Sustain. Energy Rev.*, vol. 81, pp. 2625–2636, 2018.
[57] "Real Discount Rate," Accessed: Jun. 2, 2024. [Online]. Available: https://homerenergy.com/products/pro/docs/3.15/real_discount_rate.html.

[58] "Economic and Fiscal Overview | Budget 2024," Accessed: Jun. 2, 2024. [Online]. Available: https://budget.canada.ca/2024/report-rapport/overview-apercu-en.html.
[59] S. Salisu, M. W. Mustafa, L. Olatomiwa, and O. O. Mohammed, "Assessment of technical and economic feasibility for a hybrid PV-wind-diesel-battery energy system in a remote community of north central Nigeria," *Alexandria Eng. J.*, vol. 58, no. 4, pp. 1103–1118, Dec. 2019.
[60] A. S. Aziz, "Techno-economic analysis using different types of hybrid energy generation for desert safari camps in UAE," *Turk. J. Electr. Eng. Comput. Sci.*, vol. 25, no. 3, pp. 2122–2135, 2017.
[61] S. K. A. Shezan, "Optimization and assessment of an off-grid photovoltaic–diesel–battery hybrid sustainable energy system for remote residential applications," *Environ. Prog. Sustain. Energy*, vol. 38, no. 6, p. e13340, 2019.
[62] M. Ramesh and R. P. Saini, "Dispatch strategies based performance analysis of a hybrid renewable energy system for a remote rural area in India," *J. Clean Prod.*, vol. 259, p. 120697, 2020.
[63] S. A. Shezan, K. N. Hasan, A. Rahman, M. Datta, and U. Datta, "Selection of appropriate dispatch strategies for effective planning and operation of a microgrid," *Energies*, vol. 14, no. 21, p. 7217, 2021.
[64] Statista, "Canada: monthly diesel retail price 2024," Accessed: Jun. 6, 2024. [Online]. Available: https://www.statista.com/statistics/1459287/monthly-diesel-retail-price-canada/.